A method to calibrate measurement instruments to optimise the spectrometer optics for experiment E94-107 at JLab

G. M. Urciuoli[a], E. Cisbani[b], R. De Leo[c], F. Garibaldi[b], D. W. Higinbotham[d], J. J. LeRose[e], P. Markowitz[f]

[a] *Corresponding author, address: INFN, Sezione di Roma, I-00185 Rome, Italy, email: guido.maria.urciuoli@roma1.infn.it, telephone number: (+39)-06-49914087*
[b] *INFN, Sezione di Roma and Istituto Superiore di Sanità, I-00161, Rome, Italy*
[c] *INFN, Sezione di Bari and University di Bari, I-70125, Bari, Italy*
[d] *Thomas Jefferson National Accelerator Facility, Newport News, Virginia 23606, USA*
[e] *The Chesapeake Bay Governor's School, Tappahannock, Virginia 22360, USA*
[f] *Florida International University, Miami, Florida 33199, USA*

Abstract

A method to calibrate measurement instruments through the fulfillment of physical laws is described. This method is particularly well suited to determine and/or improve magnetic spectrometer optics databases as well as to establish the best resolution achievable with them. This method was applied to obtain the best resolution achievable in the excitation and binding energy spectra of several hypernuclei produced in the experiment E94-107 performed at JLab, allowing us to obtain sub-MeV resolutions.

Keywords:
Magnetic spectrometers, Optical databases, Optimization algorithms
PACS: 29.30.-h, 29.90.+r, 41.90.+e
2010 MSC: 78A15, 78M50

1. Introduction

Obviously, if a measurement instrument is uncalibrated the measurements obtained by it cannot reproduce physical laws. In section 4.1 a simple example is given where an uncalibrated weighing scale provides mass measurements that do not fulfill Newton's law $F = M \cdot a$, with F the force a mass M

is subjected and a the mass acceleration.Moreover, if a measurement instrument is uncalibrated, physical laws show an unphysical dependence on the physical quantity it measures and possibly on the other physical quantities involved in the physical laws as well. Observing these false dependencies one is able to calibrate very precisely a measurement instrument, even using a set of samples of the physical quantity it measures whose values are completely wrong and even inventing the connection between the response of the measurement instrument and the values of the physical quantity it measures. However, the use of the method to calibrate measurement devices through the quantitative observation of the fulfillment of physical laws is not widespread. The reason for that is that it is much simpler calibrate measurement instruments using samples of the physical quantity it measures whose values are known precisely. In the case of the weighing scale quoted above, for example, instead of observing if and how much Newton's law is not fulfilled using masses whose weights are measured by it, it is much simpler to calibrate it with a sample of objects whose weights are known precisely. Nevertheless, there exist measurement instruments that cannot be calibrated using samples of known values. This is the case of databases of magnetic spectrometers employed in nuclear and high energy physics, that provide scattering coordinates of particles scattered off targets. Sometimes, when new magnetic spectrometers are employed or in case of experiments adopting old spectrometers but in kinematics completely different from the usual ones, databases are merely "invented" from scratch. The method of calibrating measurement instruments through the observation of the fulfillment of physical laws can be useful for magnetic spectrometer databases. Apart from physical laws, like the one that describes particle elastic scattering from targets, already used by experimentalists, although in a way slightly different from the one described in this paper, the physical law that most interests the experimentalists that deals with spectroscopy is the fact that energy levels, being an intrinsic feature of the nucleus under study, do not depend on scattering coordinates. Imposing the fulfillment of this law a very precise magnetic spectrometer database calibration can be obtained and maybe a little surprisingly one can even anticipate the right energy spectrum before calibrating the database. This method has been used to optimize the optics databases that determined scattering coordinates of particles detected by the two High Resolution Spectrometers used during the experiment E94-107 performed in the experimental Hall A of JLab. In a relatively fast way, this method allowed us to obtain the best resolution achievable with the spectrom-

eters, of the order of 750 MeV. In section 2 and section 3 brief descriptions of experiment E94-107 and of the magnetic High Resolution Spectrometers employed in it are given respectively. In section 4 the mathematical approach will be demonstrated, describing first a case of an uncalibrated weighing scale whose measures do not fulfill Newton's law. Although this example maybe trivial, interesting features and rules can be deduced that apply to the more complicated case of magnetic spectrometer databases treated in section 4.2. In section 5 some examples of applications of the method in the experiment E94-107 are provided.

2. The experiment E94-107

Experiment E94-107 [1] took place in Hall A at JLab (Virginia, USA). The experiment provided high resolution excitation and binding energy spectra of the hypernuclei ${}^{12}_{\Lambda}B$ [2], ${}^{16}_{\Lambda}N$ [3] and ${}^{9}_{\Lambda}Li$ [4], obtained through the reaction $e +^{A} Z \rightarrow e' + K^{+} +^{A}_{\Lambda} (Z-1)$ on ${}^{9}Be$, ${}^{12}C$ and ${}^{16}O$ targets respectively. The experiment used the JLab electron beam, whose performances are exceptional [5, 6], and two High Resolution (10^{-4}) Spectrometers (HRS), one for the detection of the scattered electrons, the other for the detection of the kaons. The trajectories of the scattered particles detected by the HRS's were focused on focal planes, where tracking chambers (two for each HRS) were installed. To allow the HRS's to detect particles scattered at angles as small as 6° two septum magnets, one for each HRS, were added to them (see section 3).

In the HRS that detected electrons, the pion rejection was performed through a gas Čerenkov detector [7] and through lead pre-shower and shower counters.

In the HRS that detected kaons, the Particle Identification System (PID) was made up by two threshold aerogel counters with refractive indices $n_1 = 1.015$ and $n_2 = 1.055$ [8, 9] and by a RICH detector [10, 11, 12, 13].

Both HRS detector packages included two planes S_1 and S_2 of 0.6×2 m^2, 2 cm thick scintillators. The detector package of the HRS that detected kaons included an additional scintillator counter S_0 (1 cm thick and with an active area of $\sim 0.19 \times 0.14$ m^2).

In 2004 the spectroscopy of the hypernuclei ${}^{12}_{\Lambda}B$ and ${}^{9}_{\Lambda}Li$ was performed. In this case the primary electron energy was 3.775 GeV and the scattered electron and the produced kaon momenta were 1.56 GeV/c and 1.96 GeV/c respectively. In 2005 the hypernucleus ${}^{16}_{\Lambda}N$ was produced performing electron scattering on a waterfall target. In this case, the primary electron energy

was 3.66 GeV and the scattered electron and the produced kaon momenta were 1.45 GeV/c and 1.96 GeV/c respectively. The presence of hydrogen in the target allowed us to simultaneously study the elementary reaction $p(e, e'K^+)\Lambda$ that, beside being interesting on its own, allowed us to calibrate very precisely the binding energy spectrum obtained as described in section 4.2.

3. The Hall A High Resolution Spectrometers

JLab Hall A is equipped with two nearly identical High Resolution Spectrometers (HRS) [14], that detect particles of momentum between 0.3 and 4 GeV/c and scattered at angles larger than 12.5°. Both HRS's bend particles vertically. Each HRS is made up of two quadrupoles followed by a dipole with a field gradient n and by a third quadrupole. Momentum, horizontal angular and vertical angular acceptances of each HRS are $\pm 4.5\%$, ± 30 mrad, and ± 60 mrad respectively. The momentum resolutions of both HRS's are smaller than 10^{-4} (FWHM), while their horizontal angular and vertical angular resolutions are 0.5 mrad and 1. mrad respectively.

During the experiment E94-107, two septa (small dipoles) were added to the HRS's (one septum for each HRS), to make them able to detect particles scattered at angles smaller than 12.5°, in order to perform measurements at low Q^2 and compensate hence the strong inverse dependence on Q^2, the squared virtual photon 4-momentum transfer, of the cross section of production of hypernuclei by electron scattering [15, 16, 17]. The septa were designed in such a way that the trajectories of particles scattered from a new target position, located 80 cm upstream, at an acceptance central angle $\phi_c = 6°$, would overlap, after being bent, the trajectories of particle scattered, inside the HRS angular acceptance, from the old target at an acceptance central angle $\phi'_c = 12.5°$. Due to their small bend angle and relatively short length (80 cm) with respect to the optical length of both HRS's, the septum magnets made only a modest perturbation on the standard HRS optics that was easily corrected by a small tuning of the three quadrupoles in each HRS.

Table 1 shows the septum magnets main features.

Eq. (1) shows the design first order transport matrix of the assembly HRS + Septum in "natural units" (meters, dimensionless, and fractional $\delta' s$).

Table 1
Septum magnets main features.

Length (including length of the coils outside the yoke)	88 cm
Height of the gap	25 cm
Width of gap entrance edge	10.4 cm
Width of gap exit edge	18.4 cm
Angular acceptance	4.7 msr
Magnetic length	84 cm

$$M_{HRS+Septum} = \begin{bmatrix} -2.81 & 0.0 & 0.0 & 0.0 & 14.06 \\ -3.19 & -0.36 & 0.0 & 0.0 & 24.69 \\ 0.0 & 0.0 & 1.01 & 0.04 & 0.13 \\ 0.0 & 0.0 & 12.81 & 1.50 & 0.52 \\ 0.0 & 0.0 & 0.0 & 0.0 & 1.0 \end{bmatrix} \tag{1}$$

$M_{HRS+Septum}$ connects, in the standard TRANSPORT formalism [18], particle scattering variables with HRS focal plane variables through the equation:

$$\vec{X}_{fp} = M_{HRS} \cdot \vec{X}_{tg} \tag{2}$$

where $\vec{X}_{fp}$ and $\vec{X}_{tg}$ are vectors whose components are the particle coordinates at HRS focal planes and target respectively:

$$\vec{X}_{fp} = \begin{pmatrix} x_{fp} \\ \theta_{fp} \\ y_{fp} \\ \phi_{fp} \\ \delta \end{pmatrix}; \qquad \vec{X}_{tg} = \begin{pmatrix} x_{tg} \\ \theta_{tg} \\ y_{tg} \\ \phi_{tg} \\ \delta \end{pmatrix} \tag{3}$$

where, in both vectors, the coordinate x represents the displacement, in the dispersive plane, of the particle trajectory with respect to the reference (central) trajectory, the angle θ is the tangent of the angle the particle trajectory makes in the dispersive plane with respect to the central trajectory, and y and ϕ are equivalent to x and θ in the transverse plane. δ is the percentage difference between the particle momentum and the spectrometer central trajectory momentum. For the HRS's x is in the vertical direction

and y is in the horizontal direction. The orientation of the x; y; and z-axes are such that $\hat{z} = \hat{x} \times \hat{y}$.

4. The mathematical method

4.1. A simple example: a weighing scale calibration through Newton's law

A measuring instrument is a device that measures a physical quantity Y pertaining a determinate object by providing a response X related to the physical quantity value by a mathematical expression $E(X)$:

$$Y = E(X) \tag{4}$$

Let us examine a very simple case: a mechanical weighing scale that provides us the mass M of an object by its spring deflection X that occurs when the object is placed on it. If we suppose that the spring deflection is proportional to the mass of the object and hence $E(X) = \alpha \cdot X$, with α constant, from eq. (4) we will have ($Y \equiv M$)

$$M = E(X) = \alpha \cdot X \tag{5}$$

A measurement instrument is uncalibrated if the real mathematical expression $R(X)$ that connects its response to the values of the physical quantity to be measured is different from the mathematical expression $E(X)$ we assume for it. For example, let us suppose that for our mechanical weighing scale quoted above the spring deflection is not proportional to the mass of the objects but follows instead the law: $R(X) = \alpha\prime \cdot X + \beta \cdot X^2 + \gamma$, with $\alpha\prime$, β, and γ constant. The real masses M_{real} of the objects measured by our mechanical weighing scale would be

$$M_{real} = R(X) = \alpha\prime \cdot X + \beta \cdot X^2 + \gamma \tag{6}$$

However, because we suppose the spring deflection proportional to the mass of the objects, and hence the validity of eq. (5), we will be provided by our weighing scale with series of measured mass values different from the real ones ($M \neq M_{real}$). In other words our weighing scale will be uncalibrated. It is very easily shown that if we try to verify Newton's law:

$$F = M \cdot A \tag{7}$$

with F the force applied to objects whose mass M is determined by our uncalibrated weighing scale through eq. (5), and A the object accelerations, we will be bitterly disappointed because we will observe instead the law:

$$F = M_{real} \cdot A = \left(\frac{\alpha\prime}{\alpha} \cdot M + \frac{\beta}{\alpha^2} \cdot M^2 + \gamma \right) \cdot A \tag{8}$$

In deriving eq. (8) we have used the equation:

$$X = \frac{M}{\alpha} \tag{9}$$

obtained by inverting eq. (5). However, the observed false mass dependence of Newton's law allows us to immediately calibrate our weighing scale. In fact, because we know that Newton's law has to be fulfilled anyway, inserting in eq. (8) the expression for M given by eq. (5), that we believe to be the relation between our weighing scale response X and the measured mass M, we obtain:

$$F = M_{real} \cdot A = \left(\frac{\alpha\prime}{\alpha} \cdot M + \frac{\beta}{\alpha^2} \cdot M^2 + \gamma \right) \cdot A =$$
$$\left(\alpha\prime \cdot X + \beta \cdot X^2 + \gamma \right) \cdot A = R(X) \cdot A \rightarrow M_{weighingscale} = R(X) \tag{10}$$

In other words we were able to derive the exact correspondence $R(X) = \alpha\prime \cdot X + \beta \cdot X^2 + \gamma$ between the spring deflection of our mechanical weighing scale and the masses it measured (that is to calibrate our mechanical weighing scale) just observing if and how Newton's law deviated from its expected behavior when we checked it using objects whose mass values were provided by our weighing scale. It can be easily shown that, similarly, if our dynamometer and/or our accelerometer by which we determined the values of forces and accelerations to be inserted in eq. (7) had been uncalibrated, we would have observed dependencies on Force and Acceleration of Newton's law that would have deviated from eq. (7) and that we would have been able to calibrate our measurement instruments correcting these unphysical dependencies.

Some comments are needed:

1. for the calibration method described in this section to be valid, the response function E(X) supposed for our measurement instrument should

be invertible. See the use of eq. (9) in eq. (10) for the case of our weighing scale. This has to always be the case, because, for the definition of the measurement instrument, to a certain response X has to correspond, within the measurement instrument resolution, only one single value of the physical quantity Y to be measured.

2. One very simple case occurs when the physical law by which our measurement instrument is calibrated can be expressed in the form

$$L(Y_1, Y_2, \ldots Y_n) = Constant \tag{11}$$

where Y_1, Y_2, $\ldots Y_n$ are physical quantities.
For example we can express Newton's law as:

$$L(F, M, A) = F - M \cdot A = 0 \tag{12}$$

In this case, if our weighing scale is calibrated (as well as our dynamometer and our accelerometer) and we plot $L(F, M, A)$ as function of M (and/or F and/or A) we will observe our measurements to be distributed around 0 with a distribution (likely Gaussian) that depends on our weighing scale resolution. Vice versa, if our weighing scale is uncalibrated, the plot of the measurements of $L(F, M, A)$, with M given by eq. (5) and M_{real} given by eq. (10) will follow the law

$$\begin{aligned} L(F, M, A) = F - M_{real} \cdot A - (F - M_{real} \cdot A - F + M \cdot A) = \\ 0 + A \cdot (M_{real} - M) = \\ A \cdot \left(\left(\frac{\alpha\prime}{\alpha} - 1 \right) \cdot M + \frac{\beta}{\alpha^2} \cdot M^2 + \gamma \right) = A \cdot P(M) \end{aligned} \tag{13}$$

where $P(M)$ is a polynomial in M. In this case, depending on the values of α, $\alpha\prime$, β and γ, the plotted values of $L(F, M, A)$ could even be centered around zero (although they usually would not) but, because of the presence of the polynomial $P(M)$ in eq. (13), their spread (that is the resolution of the measurements of the quantity $L(F, M, A)$) would be much greater than the one of the corresponding measurements obtained if our weighing scale was calibrated. In other words a calibrated measurement instrument is the one for which the resolution of the measurements of the quantity $L(Y_1, Y_2, \ldots Y_n)$ is the smallest one achievable

experimentally (principle of minimum resolution).

3. The presence of the polynomial $P(M)$ in eq. (13) is an indication (and the only indication) that our weighing scale is uncalibrated. This can be generalized: a measurement instrument measuring a physical quantity Y_n is uncalibrated if and only if the expression $L(Y_1, Y_2, \ldots Y_n) = Constant$ derived by a physical law involving several physical quantities Y_i shows a false dependence on the physical quantity Y_n. From this false dependence we are able to calibrate our measurement instrument. For example, in the case of our weighing scale, knowing that by definition

$$P(M) \equiv M_{real} - M \tag{14}$$

We can calibrate our measurement instrument, that is we can derive the expression (6) of M_{real} as function of X (see eq. (5), eq. (13), and eq. (14)):

$$\begin{aligned} M_{real} = M + (M_{real} - M) = M + P(M) = \\ M + \left(\left(\frac{\alpha\prime}{\alpha} - 1 \right) \cdot M + \frac{\beta}{\alpha^2} \cdot M^2 + \gamma \right) = \\ \alpha \cdot X + \left(\left(\frac{\alpha\prime}{\alpha} - 1 \right) \cdot (\alpha \cdot X) + \frac{\beta}{\alpha^2} \cdot (\alpha \cdot X)^2 + \gamma \right) = \\ \alpha' \cdot X + \beta \cdot X^2 + \gamma = R(X) \end{aligned} \tag{15}$$

To calibrate a measurement instrument that measures a physical quantity Y_n which is involved in a physical law "at hand", whose analytical expression is given by eq. (11), it is "sufficient" hence to plot eq. (11) as function of Y_n and observe the dependence of $L(Y_1, Y_2, \ldots Y_n)$ on Y_n. The calibration of the measurement instrument is then straightforward.

4. From what is described above, it is obvious that if law (11) does not show any false dependence on Y_n, the instrument measuring Y_n is calibrated and no further attempt to improve its measurements should be performed. In fact, in this case, the relationship $Y = E(X)$ that we suppose exists between the response X of our measurement instrument and the value Y of the physical quantity measured is coincident

with the real/right one $Y = R(X)$ within the instrument precision. In other words, $E(X) = R(X)$. Any attempt to modify $E(X)$ will cause $E(X) \neq R(X)$ and will consequently generate a false dependence of law (11) on Y_n.

4.2. Optical databases of magnetic spectrometers

A magnetic spectrometer determines momentum, coordinates, and direction of a particle scattered off a target through the mathematical relationship between these variables and the coordinates and direction of the scattered particle as measured at the magnetic spectrometer focal plane

$$\vec{Y} = T \cdot \vec{X} \tag{16}$$

where $\vec{Y}$ is the vector composed of δ, the percentage difference between the particle momentum and the momentum of the spectrometer central trajectory, y_0 the position along the target of the particle scattering point, and θ_0 and ϕ_0, the tangents of the angles that identify the particle direction just after its scattering off the target

$$\vec{Y} = \begin{pmatrix} \delta \\ y_0 \\ \theta_0 \\ \phi_0 \end{pmatrix} \tag{17}$$

and $\vec{X}$ is the vector made up by the particle coordinates x_f and y_f at the focal plane and by θ_f and ϕ_f that are the tangents of the angles that define the particle trajectory when it hits the focal plane

$$\vec{X} = \begin{pmatrix} x_f \\ y_f \\ \theta_f \\ \phi_f \end{pmatrix} \tag{18}$$

y_0, θ_0, ϕ_0, x_f, y_f, θ_f, and ϕ_f are measured with respect to the corresponding parameters of the central trajectory inside the spectrometer and hence are equal to zero for a particle whose trajectory coincides with the spectrometer central trajectory. The same is true for δ as can be deduced by its definition given above. As in a spectrometer the deviations of particle parameters with respect to the corresponding central trajectory are usually

small, the angles that define particle trajectories with respect to the spectrometer central trajectory are very small and nearly numerically equal to their tangents. For this reason, for the sake of simplicity, we refer in this paper to θ_0, ϕ_0, θ_f, and ϕ_f as angles, although they are actually the tangents of the angles they are identified with. It has to be noted at last that, because the variables that can be measured at the focal plane are four (x_f, y_f, θ_f, and ϕ_f), only four of the five scattering variables (δ, x_0, y_0, θ_0, and ϕ_0) can be deduced by them. Usually, the scattering variable that is not deduced from the four focal plane variables is x_0 which is made coincident with the (usually very small) dimension of the particle primary beam along the spectrometer dispersion direction. The impossibility to derive x_0 determines the first order magnetic spectrometer resolution.

T is the tensor that allows us to derive $\vec{Y}$ from $\vec{X}$. We can express the single elements Y_i of the vector $\vec{Y}$ as Taylor's series in the elements X_i of the vector $\vec{X}$. Eq. (16) has hence the form:

$$Y_i = \sum_{klmn} T_{iklmn} \cdot (X_1)^k \cdot (X_2)^l \cdot (X_3)^m \cdot (X_4)^n \tag{19}$$

where $i = 1, 2, 3, 4$; k, l, m, and n are integer numbers, and T_{iklmn} are real numbers.

As in a spectrometer the deviation of particle parameters are usually small with respect to the corresponding central trajectory, the series of eq. (19) can usually be truncated at relatively small values of k, l, m, and n within a very good approximation. In the first order approximation, eq. (19) becomes the usual matrix algebra rule:

$$Y_i = \sum_{j=1,4} T_{ij} \cdot X_j \tag{20}$$

T is called the "Optical database" of the magnetic spectrometer.

Beside dealing with vectors instead of scalars, eq. (16) is formally identical to eq. (4) and hence all the considerations for the method described in section 4.1 to check if our weighing scale was uncalibrated and to calibrate it in that case apply as well (see items i-iv at the end of section 4.1). In particular, we can optimize the optical database (in other words we can calibrate it) looking for possible unphysical dependence on the variables Y_i of physical laws of the kind

$$L(Y_1, Y_2, Y_3, Y_4) \equiv L(\delta, y_0, \theta_0, \phi_0) = constant \tag{21}$$

There are several of them.

One is the elastic scattering formula:

$$E' - \frac{E_0}{1 + \frac{E_0}{M} \cdot (1 - \cos(\Theta))} = 0 \tag{22}$$

where E_0 and E' are the energy of the particle before and after the scattering respectively, Θ is the particle scattering angle, and M is the mass of the nucleus the particle scatters off. Obviously, E' and Θ can be expressed as function of δ, and δ, θ_0 and ϕ_0 respectively (see Appendix Appendix B for their explicit expressions in the case of the coordinate system adopted with the High Resolution Spectrometers used in the experiment E94-107), while E_0 is known as provided by the particle accelerator setup. Eq. (22) has hence the form:

$$L(\delta, \theta_0, \phi_0) = 0 \tag{23}$$

Another two eq. (21)-like laws are:

$$\theta_0 = constant_\theta \tag{24}$$

and

$$\phi_0 = constant_\phi \tag{25}$$

that have to be fulfilled by the angles θ_0 and ϕ_0, that define the direction of scattered particles, when a sieve slit is placed in front of the magnetic spectrometer in order to make it detect particles scattered only at defined couples of angles $(constant_\theta, constant_\phi)$.

An additional law is:

$$y_0 = constant_y \tag{26}$$

This has to be fulfilled when particles scatter off a point-like target, positioned at a definite position $constant_y$ along the beam line.

A fifth law exists for experiments that detect particles in coincidence in order to perform nuclear and/or hypernuclear spectroscopy as the experiment E94-107 at JLab. This law is maybe the most interesting for this kind of experiments and can be enunciated as follows: nuclear and/or hypernuclear energy levels are an intrinsic property of the nucleus/hypernucleus under study and cannot depend on the direction and momenta of scattered particles.

In other words, defining E_{bind_n} the binding energy of the nth energy state of a nucleus/hypernucleus, we have to have:

$$E_{bind_n} = constant_n \tag{27}$$

Checking possible unphysical dependences on scattering coordinates of physical laws of the kind of eq. (21) it is possible to calibrate a magnetic spectrometer. In this paper the general case of experiments that for each event detect by two magnetic spectrometers, two particles in coincidence (the secondary electron e' and the produced kaon k in the case of the experiment E94-107), whose scattering coordinates are identified by the subscripts e' and k respectively, will be considered. We assume for the sake of simplicity in the following that only the database relative to the spectrometer that detects the particle e' is uncalibrated. By an obvious generalization, the results obtained can be easily applied to the case in which the spectrometer that detects the particle k is also uncalibrated.

As eq. (A.10) shows, it is possible to express the numerical change $\Delta Y_{e'_i}$, which the ith scattering coordinate $Y_{e'_i}$ of the particle e' is subjected due to a change of the spectrometer optical database $T_{e'}$, as a polynomial in the scattering coordinates $Y_{e'_i}$ themselves. As demonstrated in Appendix Appendix A this is due to the fact that eq. (16) is invertible:

$$\vec{X}_{e'} = T_{e'}^{-1} \cdot \vec{Y}_{e'} \tag{28}$$

with $T_{e'}^{-1}$ the inverse of the matrix/tensor $T_{e'}$. The existence of $T_{e'}^{-1}$ is guaranteed by considerations similar to those in comment "i" at the end of section 4.1.

The possibility of expressing as polynomials in the scattering coordinates $Y_{e'_i}$, as determined by an old database $T_{e'}$, the numerical changes the scattering coordinates themselves are subjected as a result of a change of the spectrometer optical database $T_{e'}$, has important consequences. In fact, when $T_{e'}$ is changed, the numerical values of $L(\delta_{e'}, y_{e'_0}, \theta_{e'_0}, \phi_{e'_0})$ in eq. (21) change into:

$$L(\delta_{e'}, y_{e'_0}, \theta_{e'_0}, \phi_{e'_0}) \rightarrow L(\delta_{e'}, y_{e'_0}, \theta_{e'_0}, \phi_{e'_0}) + P(\delta_{e'}, y_{e'_0}, \theta_{e'_0}, \phi_{e'_0}) \tag{29}$$

where $P(\delta_{e'}, y_{e'_0}, \theta_{e'_0}, \phi_{e'_0})$ is a polynomial in the particle e' scattering coordinates $\delta_{e'}$, $y_{e'_0}$, $\theta_{e'_0}$, and $\phi_{e'_0}$ (see eq. (A.12) and eq. (A.16), remembering that according to our definition $Y_{e'_1} \equiv \delta_{e'}$, $Y_{e'_2} \equiv y_{e'_0}$, $Y_{e'_3} \equiv \theta_{e'_0}$, and $Y_{e'_4} \equiv \phi_{e'_0}$, and that $L(\delta_{e'}, y_{e'_0}, \theta_{e'_0}, \phi_{e'_0}) \equiv \theta_{e'_0}$ in eq. (24), $L(\delta_{e'}, y_{e'_0}, \theta_{e'_0}, \phi_{e'_0}) \equiv \phi_{e'_0}$ in eq.

(25), $L(\delta_{e'}, y_{e'_0}, \theta_{e'_0}, \phi_{e'_0}) \equiv y_{e'_0}$ in eq. (26), and $L(\delta_{e'}, y_{e'_0}, \theta_{e'_0}, \phi_{e'_0}) \equiv E_{bind_n}$ in eq. (27)). All one has to do to check if a spectrometer optical database is calibrated is to plot, vs the other scattering variables, profile histograms of each of the scattering variables $y_{e'_0}$, $\theta_{e'_0}$, and $\phi_{e'_0}$ as determined by the database when particles e' enter the sieve slit hole corresponding to the scattering angles $(constant_\theta, constant_\phi)$ and are scattered off a target located at the point $y = constant_y$, as well as to plot profile histograms of the nuclear energy level values determined in the whole experiment vs the scattering variables. If these histograms show no dependence on scattering variables (in other words if they are constant within the spectrometer resolution) eq. (24), eq. (25), eq. (26), and eq. (27) are fulfilled and hence the spectrometer database is optimized. No attempt to improve it should be performed. In fact, any change in it will result in an addition of polynomials in scattering coordinates to $constant_\theta$, $constant_\phi$, $constant_y$ and $constant_n$ in eq. (24), eq. (25), eq. (26), and eq. (27). These equations will hence not be fulfilled (see eq. (29) and comment "iv" at the end of section 4.1). If, on the other hand, the spectrometer optical database is uncalibrated, the profile histograms quoted above will show that eq. (24), eq. (25), eq. (26), and eq. (27) will be not fulfilled but will have the form:

$$\begin{aligned} y_{e'_0} &= constant_y + P_y(\delta_{e'}, y_{e'_0}, \theta_{e'_0}, \phi_{e'_0}) \\ \theta_{e'_0} &= constant_\theta + P_\theta(\delta_{e'}, y_{e'_0}, \theta_{e'_0}, \phi_{e'_0}) \\ \phi_{e'_0} &= constant_\phi + P_\phi(\delta_{e'}, y_{e'_0}, \theta_{e'_0}, \phi_{e'_0}) \\ E_{bind_n} &= constant_n + P_{E_{bind_n}}(\delta_{e'}, y_{e'_0}, \theta_{e'_0}, \phi_{e'_0}) \end{aligned} \tag{30}$$

with $P_y(\delta_{e'}, y_{e'_0}, \theta_{e'_0}, \phi_{e'_0})$, $P_\theta(\delta_{e'}, y_{e'_0}, \theta_{e'_0}, \phi_{e'_0})$, $P_\phi(\delta_{e'}, y_{e'_0}, \theta_{e'_0}, \phi_{e'_0})$, and $P_{E_{bind_n}}(\delta_{e'}, y_{e'_0}, \theta_{e'_0}, \phi_{e'_0})$ polynomials in $\delta_{e'}$, $y_{e'_0}$, $\theta_{e'_0}$, and $\phi_{e'_0}$. However, in this case, using the method described in this paper, the spectrometer database calibration will be straightforward. In fact, the calibration of the database terms $T_{e'_{2klmn}}$, $T_{e'_{3klmn}}$, and $T_{e'_{4klmn}}$ that provide the scattering variables $y_{e'_0}$, $\theta_{e'_0}$, and $\phi_{e'_0}$ respectively through eq. (19) is obtained observing that the new scattering variables:

$$\begin{aligned} y'_{e'_0} &= y_{e'_0} - P_y(\delta_{e'}, y_{e'_0}, \theta_{e'_0}, \phi_{e'_0}) \\ \theta'_{e'_0} &= \theta_{e'_0} - P_\theta(\delta_{e'}, y_{e'_0}, \theta_{e'_0}, \phi_{e'_0}) \\ \phi'_{e'_0} &= \phi_{e'_0} - P_\phi(\delta_{e'}, y_{e'_0}, \theta_{e'_0}, \phi_{e'_0}) \end{aligned} \tag{31}$$

fulfill eq. (24), eq. (25), and eq. (26). Expressing in eq. (31), through eq. (19), $\delta_{e'}$, $y_{e'_0}$, $\theta_{e'_0}$, and $\phi_{e'_0}$ as a function of $x_{e'_f}$, $y_{e'_f}$, $\theta_{e'_f}$, and $\phi_{e'_f}$, we obtain the equation:

$$
\begin{aligned}
y'_{e'_0} &= \sum_{klmn} T'_{e'_{2klmn}} \cdot \left(x_{e'_f}\right)^k \cdot \left(y_{e'_f}\right)^l \cdot \left(\theta_{e'_f}\right)^m \cdot \left(\phi_{e'_f}\right)^n \\
\theta'_{e'_0} &= \sum_{klmn} T'_{e'_{3klmn}} \cdot \left(x_{e'_f}\right)^k \cdot \left(y_{e'_f}\right)^l \cdot \left(\theta_{e'_f}\right)^m \cdot \left(\phi_{e'_f}\right)^n \\
\phi'_{e'_0} &= \sum_{klmn} T'_{e'_{4klmn}} \cdot \left(x_{e'_f}\right)^k \cdot \left(y_{e'_f}\right)^l \cdot \left(\theta_{e'_f}\right)^m \cdot \left(\phi_{e'_f}\right)^n
\end{aligned} \tag{32}
$$

The coefficients $T'_{e'_{2klmn}}$, $T'_{e'_{3klmn}}$, and $T'_{e'_{4klmn}}$ of eq. (32) are just the terms of the calibrated database we were looking for because they provide the calibrated scattering variables $y'_{e'_0}$, $\theta'_{e'_0}$, and $\phi'_{e'_0}$ of eq. (31) that fulfill eq. (24), eq. (25), and eq. (26).

The calibration of the database terms $T_{e'_{1klmn}}$ that provide the scattering variable $\delta_{e'}$ is obtained by a conceptually similar although slightly more complicated method.

It is easily shown that if the terms $T_{e'_{1klmn}}$ of the spectrometer optical database that provide the scattering variable $\delta_{e'}$ through eq. (19) are not calibrated, the binding energies E_{bind_n} do not follow eq. (27) even using for their calculation the calibrated scattering variables $y'_{e'_0}$, $\theta'_{e'_0}$, and $\phi'_{e'_0}$ of eq. (31) and eq. (32), but the equation:

$$
\begin{aligned}
&E_{bind_n}(\delta_{e'}, y'_{e'_0}, \theta'_{e'_0}, \phi'_{e'_0}, \delta_k, y_{k_0}, \theta_{k_0}, \phi_{k_0}) = \\
&\quad constant_n + P'_{E_{bind_n}}(\delta_{e'}, y'_{e'_0}, \theta'_{e'_0}, \phi'_{e'_0})
\end{aligned} \tag{33}
$$

where δ_k, y_{k_0}, θ_{k_0}, and ϕ_{k_0} are the particle k scattering coordinates determined by the optical database T_k supposedly calibrated and $P'_{E_{bind_n}}(\delta_{e'}, y'_{e'_0}, \theta'_{e'_0}, \phi'_{e'_0})$ is the polynomial:

$$
P'_{E_{bind_n}}(\delta_{e'}, y'_{e'_0}, \theta'_{e'_0}, \phi'_{e'_0}) = \sum_{klmn} C_{e'_{1klmn}} \cdot (\delta_{e'})^k \cdot \left(y'_{e'_0}\right)^l \cdot \left(\theta'_{e'_0}\right)^m \cdot \left(\phi'_{e'_0}\right)^n \tag{34}
$$

(eq. (34) derived from eq. (A.13), eq. (A.16), and eq. (A.16) with $\Delta Y^1_{e'_2} = \Delta Y^1_{e'_3} = \Delta Y^1_{e'_4} = 0$ and supposing $T^1_{e'}$ a calibrated database). The

real coefficients $C_{e'_{1klmn}}$ can be easily determined plotting profile histograms of E_{bind_n} vs $\delta_{e'}$, $y'_{e'_0}$, $\theta'_{e'_0}$, and $\phi'_{e'_0}$.

It can be demonstrated that the binding energies E_{bind_n} follow eq. (27) if the variable $\delta_{e'}$ is replaced by the variable $\delta'_{e'}$ defined as:

$$\delta'_{e'} = \delta_{e'} - \sum_{klmn} U_{e'_{1klmn}} \cdot (\delta_{e'})^k \cdot \left(y'_{e'_0}\right)^l \cdot \left(\theta'_{e'_0}\right)^m \cdot \left(\phi'_{e'_0}\right)^n \tag{35}$$

with the coefficients $U_{e'_{1klmn}}$ related to the coefficients $C_{e'_{1klmn}}$ by the relationship:

$$C_{e'_{1klmn}} = U_{e'_{1klmn}} \cdot \frac{\partial E_{bind_n}}{\partial \delta_{e'}} \tag{36}$$

(the demonstration is derived from eq. (A.13) and eq. (A.16), with $\Delta Y^1_{e'_2} = \Delta Y^1_{e'_3} = \Delta Y^1_{e'_4} = 0$, supposing $T^1_{e'}$ a calibrated database and noting that the calibrated variable $Y^1_{e'_1}$ is equal to $Y^2_{e'_1} - \Delta Y^1_{e'_1}$, with $\Delta Y^1_{e'_1}$ provided by eq. (A.10)). To determine the terms $U_{e'_{1klmn}}$ without calculating $\frac{\partial E_{bind_n}}{\partial \delta_{e'}}$, one can define, for each term $C_{e'_{1klmn}} \cdot (\delta_{e'})^k \cdot \left(y'_{e'_0}\right)^l \cdot \left(\theta'_{e'_0}\right)^m \cdot \left(\phi'_{e'_0}\right)^n$ of the polynomial $P'_{E_{bind_n}}$ of eq. (34), the variable

$$\begin{aligned} E_{bind_n}(\delta_{e'} + \alpha \cdot (\delta_{e'})^k \cdot \left(y'_{e'_0}\right)^l \cdot \left(\theta'_{e'_0}\right)^m \cdot \left(\phi'_{e'_0}\right)^n, \\ y'_{e'_0}, \theta'_{e'_0}, \phi'_{e'_0}, \delta_k, y_{k_0}, \theta_{k_0}, \phi_{k_0}) = \\ E_{bind_n}(\delta_{e'}, y'_{e'_0}, \theta'_{e'_0}, \phi'_{e'_0}, \delta_k, y_{k_0}, \theta_{k_0}, \phi_{k_0}) + \\ K \cdot (\delta_{e'})^k \cdot \left(y'_{e'_0}\right)^l \cdot \left(\theta'_{e'_0}\right)^m \cdot \left(\phi'_{e'_0}\right)^n \end{aligned} \tag{37}$$

with α an arbitrary real number and with

$$K = \alpha \cdot \frac{\partial E_{bind_n}}{\partial \delta_{e'}} \tag{38}$$

(eq. (37) is derived from eq. (A.13) with $\Delta Y^1_{e'_2} = \Delta Y^1_{e'_3} = \Delta Y^1_{e'_4} = 0$ and $\Delta Y^1_{e'_1} = \alpha \cdot (\delta_{e'})^k \cdot \left(y'_{e'_0}\right)^l \cdot \left(\theta'_{e'_0}\right)^m \cdot \left(\phi'_{e'_0}\right)^n$).

Eq. (37) can be written as:

$$E_{bind_n}(\delta_{e'} + \alpha \cdot (\delta_{e'})^k \cdot \left(y'_{e'_0}\right)^l \cdot \left(\theta'_{e'_0}\right)^m \cdot \left(\phi'_{e'_0}\right)^n, \\ y'_{e'_0}, \theta'_{e'_0}, \phi'_{e'_0}, \delta_k, y_{k_0}, \theta_{k_0}, \phi_{k_0}) - \\ E_{bind_n}(\delta_{e'}, y'_{e'_0}, \theta'_{e'_0}, \phi'_{e'_0}, \delta_k, y_{k_0}, \theta_{k_0}, \phi_{k_0}) = \\ K \cdot (\delta_{e'})^k \cdot \left(y'_{e'_0}\right)^l \cdot \left(\theta'_{e'_0}\right)^m \cdot \left(\phi'_{e'_0}\right)^n \tag{39}$$

Determining K from a profile histogram of the term on the left vs the term on the right side of the sign "=" in eq. (39), from eq. (38) and eq. (36) we have:

$$U_{e'_{1klmn}} = \frac{\alpha}{K} \cdot C_{e'_{1klmn}} \tag{40}$$

Once the coefficients $U_{e'_{1klmn}}$ are determined, expressing in eq. (35), through eq. (19) and eq. (32)), $\delta_{e'}$, $y'_{e'_0}$, $\theta'_{e'_0}$, and $\phi'_{e'_0}$ as function of $x_{e'_f}$, $y_{e'_f}$, $\theta_{e'_f}$, and $\phi_{e'_f}$, we obtain the equation:

$$\delta'_{e'} = \sum_{klmn} T'_{e'_{1klmn}} \cdot \left(x_{e'_f}\right)^k \cdot \left(y_{e'_f}\right)^l \cdot \left(\theta_{e'_f}\right)^m \cdot \left(\phi_{e'_f}\right)^n \tag{41}$$

The coefficients $T'_{e'_{1klmn}}$ of eq. (41) are just the terms of the calibrated database providing the values of $\delta'_{e'}$ we are looking for.
A complementary way to derive the terms $T'_{e'_{1klmn}}$ is to check the fulfillment of the law that connects momentum and scattering angle of an elastic scattered particle, that is eq. (22), that can be expressed as function of $\delta_{e'}$, $\theta_{e'_0}$, and $\phi_{e'_0}$ as shown in Appendix Appendix B for the case of the coordinate system adopted for the High Resolution Spectrometers used in the experiment E94-107. For elastic electron scattering, in the case of a target with a mass much bigger than the energy of the primary beam:

$$M \gg E_0 \tag{42}$$

we have (in a unit system where c = 1)

$$\delta_{e'} \approx \frac{E_0}{P_{e'_c}} - 1 = constant_\delta \tag{43}$$

with $P_{e'_c}$ the central trajectory momentum of the spectrometer. In this case, the method to determine $T'_{e'_{2klmn}}$, $T'_{e'_{3klmn}}$, and $T'_{e'_{4klmn}}$ described above

applies to the determination of $T'_{e'_{1klmn}}$ as well and we can check for a possible dependence of $\delta_{e'}$ on scattering coordinates of the kind:

$$\delta_{e'} = constant_{\delta} + P_{\delta}(\delta_{e'}, y_{e'_0}, \theta_{e'_0}, \phi_{e'_0}) \tag{44}$$

with $P_{\delta}(\delta_{e'}, y_{e'_0}, \theta_{e'_0}, \phi_{e'_0})$ a polynomial in the scattering coordinates. If the dependence, expressed by eq. (44), of $\delta_{e'}$ on scattering coordinates exists, then the determination of $T'_{e'_{1klmn}}$ will be done observing that the new variable $\delta'_{e'}$ defined as:

$$\delta'_{e'} = \delta_{e'} - P_{\delta}(\delta_{e'}, y_{e'_0}, \theta_{e'_0}, \phi_{e'_0}) = \sum_{klmn} T'_{e'_{1klmn}} \cdot \left(x_{e'_f}\right)^k \cdot \left(y_{e'_f}\right)^l \cdot \left(\theta_{e'_f}\right)^m \cdot \left(\phi_{e'_f}\right)^n \tag{45}$$

fulfills eq. (43) (see eq. (31) and eq. (32)). If the approximation of eq. (42) is not valid, or if we want a more precise determination of $T'_{e'_{1klmn}}$, we can use the same method to determine $T'_{e'_{1klmn}}$ measuring binding energies in the coincidence experiments described above, substituting in eq. (33), eq. (36), and eq. (37) E_{bind_n} with $E' - \frac{E_0}{1+\frac{E_0}{M}\cdot(1-\cos(\Theta))}$.
The spectrometer database optimization method described in this paper is based on the search of "calibrated" scattering variables $\delta'_{e'}$, $y'_{e'_0}$, $\theta'_{e'_0}$, and $\phi'_{e'_0}$ that fulfill eq. (22), eq. (24), eq. (25), eq. (26), and eq. (27). These calibrated scattering variables are obtained by the addition of polynomials in scattering coordinates to the "uncalibrated" scattering variables $\delta_{e'}$, $y_{e'_0}$, $\theta_{e'_0}$, and $\phi_{e'_0}$, derived by our original and uncalibrated spectrometer database (see eq. (35), eq. (45), and eq. (31)). These polynomials can be derived by profile histograms as quoted above, or, alternatively, making use of the principle of minimum resolution described in comment "ii" at the end of the section 4.1. In fact, these polynomials can be derived by histogramming $y_{e'_0}$, $\theta_{e'_0}$, $\phi_{e'_0}$, E_{bind_n}, and $\delta_{e'}$, that is the variables on the left side of the sign "=" in eq. (24), eq. (25), eq. (26), eq. (27), and eq. (43), that would be constant within the spectrometer resolution if the spectrometer database was calibrated. If one of these variables is uncalibrated, we will find polynomial terms of the kind: $C_{e'_{iklmn}} \cdot (\delta_{e'})^k \cdot \left(y_{e'_0}\right)^l \cdot \left(\theta_{e'_0}\right)^m \cdot \left(\phi_{e'_0}\right)^n$ (or $C_{e'_{1klmn}} \cdot (\delta_{e'})^k \cdot \left(y'_{e'_0}\right)^l \cdot \left(\theta'_{e'_0}\right)^m \cdot \left(\phi'_{e'_0}\right)^n$ for the binding energies) that when added to it will decrease the variable histogram FWHM and consequently will increase the histogram height, while

keeping at the same time the center of the histogram at the expected positions. The sum of all the polynomial terms determined this way will provide the polynomials $P_y(\delta_{e'}, y_{e'_0}, \theta_{e'_0}, \phi_{e'_0})$, $P_\theta(\delta_{e'}, y_{e'_0}, \theta_{e'_0}, \phi_{e'_0})$, $P_\phi(\delta_{e'}, y_{e'_0}, \theta_{e'_0}, \phi_{e'_0})$, $P'_{E_{bind_n}}(\delta_{e'}, y'_{e'_0}, \theta'_{e'_0}, \phi'_{e'_0})$, and $P_\delta(\delta_{e'}, y_{e'_0}, \theta_{e'_0}, \phi_{e'_0})$ of eq. (31), eq. (33), and eq. (45) we are looking for because the histogram of the variables made up by the addition of these polynomials to the corresponding uncalibrated variables $y_{e'_0}$, $\theta_{e'_0}$, $\phi_{e'_0}$, E_{bind_n}, and $\delta_{e'}$ are constant (that is they have the minimum FWHM and maximum height achievable) within the spectrometer resolution and hence fulfill eq. (22), eq. (24), eq. (25), eq. (26), and eq. (27).
We stress that, while it is surely desirable to produce the calibrated database $T'_{e'}$, it is not necessary to know explicitly its terms $T'_{e'_{iklmn}}$ to perform the measurements. For example, in experiments aimed at measuring the binding energies of the ground and excited states of nuclei and/or hypernuclei, the binding energies can be determined replacing, in their calculation, the uncalibrated variables $\delta_{e'}$, $\theta_{e'_0}$, and $\phi_{e'_0}$ with the new variables $\delta_{e'}$, $\theta'_{e'_0}$, and $\phi'_{e'_0}$, determined through eq. (35) and eq. (31) and that can hence be derived without determining the coefficients $T'_{e'_{iklmn}}$ of the calibrated spectrometer database. The mathematical reason for that is the fact that performing calculations using as a base the coordinates at the focal planes (that is the components of $\vec{X}$) is equivalent to performing calculations using as a base the coordinates at the scattering point (that is the components of $\vec{Y}$) because of relationships (16) and (28). After calibrating the coordinates at the scattering point with the methods described above, we can perform calculations using them directly and there is no need to again represent variables as functions of the coordinates at focal planes. Going further in this direction, we can say that the correct binding energies can be obtained even without determining the calibrated scattering variables $\delta_{e'}$, $\theta'_{e'_0}$, and $\phi'_{e'_0}$ through eq. (35) and eq. (31). In fact, if in plotting profile histograms we realize that the measured binding energies E_{bind_n} do not fulfill eq. (27) but instead the equation

$$\begin{aligned} E_{bind_n}(\delta_{e'}, y_{e'_0}, \theta_{e'_0}, \phi_{e'_0}, \delta_k, y_{k_0}, \theta_{k_0}, \phi_{k_0}) = \\ constant_n + P_{E_{bind_n}}(\delta_{e'}, y_{e'_0}, \theta_{e'_0}, \phi_{e'_0}) \end{aligned} \tag{46}$$

we already know that the correct values of the binding energies are those obtained subtracting the polynomial $P_{E_{bind_n}}(\delta_{e'}, y_{e'_0}, \theta_{e'_0}, \phi_{e'_0})$ from the binding

energies determined with the present uncalibrated spectrometer database. At last we have to remember that optical databases provide scattering coordinates relative to the spectrometer central trajectory. So far we have supposed the central trajectory momentum $P_{e'_c}$ and scattering angles $\theta_{e'_c}$ and $\phi_{e'_c}$ of the spectrometer that detects the particle e' as well as the corresponding parameters P_{k_c}, θ_{k_c}, and ϕ_{k_c} of the spectrometer that detects the particle k are perfectly known in the laboratory frame. If this is not true binding energy spectra will be uncalibrated. The values of a spectrometer central trajectory momentum and scattering angles are usually derived from measurements that have nothing to do with the spectrometer database, as the measurements of the fields of the magnetic elements that make up the spectrometer and the measurement of the position of the spectrometer axis with respect to the direction of the primary beam. However, a much more precise measurement can be performed checking the binding energy spectrum obtained. In fact, as demonstrated in Appendix B of ref. [4], the fact that the nominal values of the spectrometer central trajectory momenta and scattering angles, as well as that of the primary beam energy, differ from their actual and unknown values has two effects: 1) it causes a global shift of the positions, in the binding energy spectrum, of the peaks corresponding to the energy levels of the nucleus/hypernucleus under study; 2) it causes a dependence on scattering coordinates of the calculated binding energies. This second feature is not surprising, because the fact that a spectrometer's actual central trajectory momentum and scattering angles differ from their nominal values means that the spectrometer database, although maybe calibrated when deriving scattering coordinates with respect to the central trajectory, is not calibrated when these variables are computed in the laboratory frame, because of the fact that the central trajectory coordinates are uncalibrated as well. To lessen this problem, experiment E94-107 derived the best estimate of the spectrometer central trajectory momenta and scattering angles and of the primary beam energy positioning, in the binding energy spectrum, the peaks corresponding to binding energies of well known energy levels at their known position and simultaneously minimizing the peak FWHMs. For the study of the hypernucleus ${}^{16}_{\Lambda}N$, the peaks used for binding energy spectrum calibration were the peak of the reaction $p(e, e'K^+)\Lambda$ that had to be positioned at 0 (see eq. (C.2) with $M_{residue} = 0$) and the peak of the reaction $p(e, e'K^+)\Sigma$ that had to be positioned at the value corresponding to the mass difference between the particles Σ and Λ. For the study of the hypernucleus ${}^{9}_{\Lambda}Li$, the peak used for binding energy spectrum calibration was the ground

state of the hypernucleus ${}^{12}_{\Lambda}B$, that had to be located at the well known value of 11.37 ± 0.06 MeV. See ref. [4] for more details.

5. The method applied for the optimization of the databases of the Hall A High Resolution Spectrometers

Avoiding describing in too much detail the several steps used in the optimization of the optical databases of the two Hall A High Resolution Spectrometers (referred in the following as the right HRS and the left HRS respectively) during experiment E94-107 analysis, just one example showing most of the concepts described in section 4.2 will be given. Figure 1 shows the two-dimensional histogram of the scattering variables θ and ϕ (referred as θ_0 and ϕ_0 in section 4.2) as reconstructed by the still to be optimized database of the right HRS when a sieve slit was placed in front of the spectrometer during a calibration run performed detecting electrons scattered elastically off a very thin ${}^{12}C$ target. The sieve slit was a shield with holes drilled such that only electrons whose direction after being scattered was defined by specific couples of values $(constant_\theta, constant_\phi)$ could pass the shield and be detected by the spectrometer. The sieve slit hole structure is evident from the plot that shows "spots" corresponding to the hole positions in the sieve slit.

Figure 2 shows the histogram of θ only. There are seven peaks corresponding to the seven θ values of the spot centers of Figure 1. It can be shown that the reconstruction of θ by the right HRS database cannot be improved. In fact, any plot of variables of the kind $\theta + P_\theta(\delta, y, \theta, \phi)$, with $P_\theta(\delta, y, \theta, \phi)$ a polynomial in scattering coordinates, would decrease the heights of Figure 2 peaks and increase their widths.

The situation is different in the case of the scattering variable ϕ. Figure 3a shows the histogram of ϕ. Six peaks are present corresponding to the six ϕ values of the spot centers of Figure 1. Figure 3b shows that when plotting the variable $\phi - P_\phi$, with $P_\phi = 0.042 \cdot \delta + 0.57 \cdot \delta^2 + 0.002 \cdot \theta - 0.8 \cdot \theta^2 - 0.18 \cdot y + 15.9 \cdot y^2 - 1.3 \cdot \theta \cdot \phi$, the peaks are higher and thinner than the corresponding peaks of Figure 3a and then that the peak resolution in Figure 3b is better than in Figure 3a. This means that the law $\phi = constant_n$, with $n = 1, 2, \ldots 6$ and $constant_n$ being one of the six ϕ values of Figure 1 spot centers, is not fulfilled by the electrons detected by the right HRS if ϕ is determined by the original database of this spectrometer. The law $\phi - P_\phi = constant_n$ is fulfilled instead. As explained in section 4.2, this shows that the terms of the right

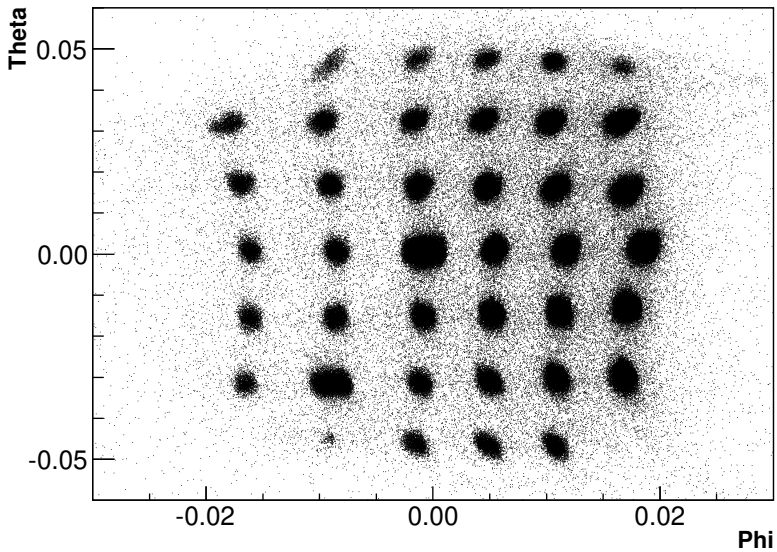

Figure 1: θ vs ϕ plot obtained with the right HRS database during a calibration run performed through electron elastic scattering off a ^{12}C target with a sieve slit placed in front of the spectrometer.

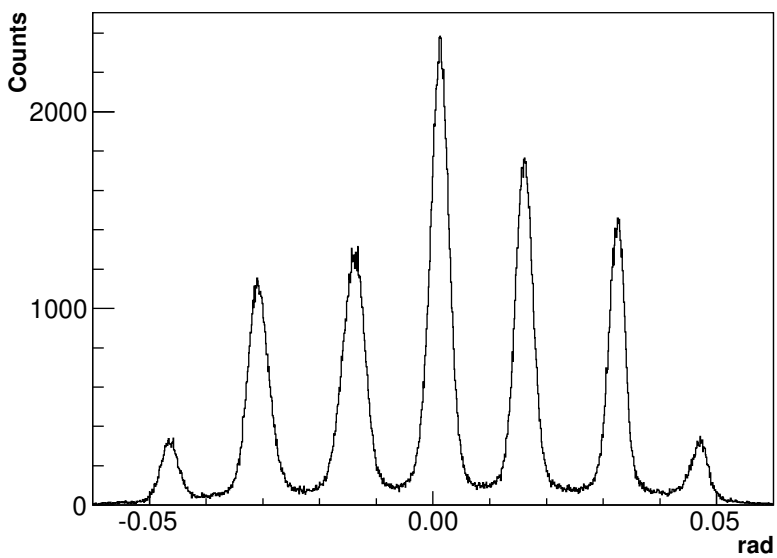

Figure 2: Scattering variable θ histogram as derived by Figure 1.

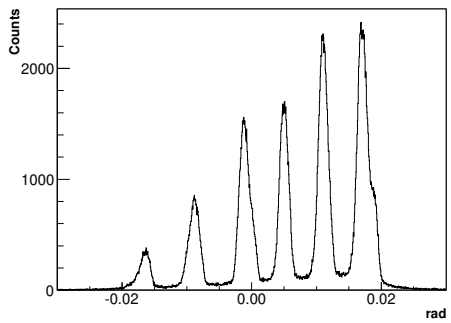

(a) Scattering variable ϕ histogram as derived by Figure 1.

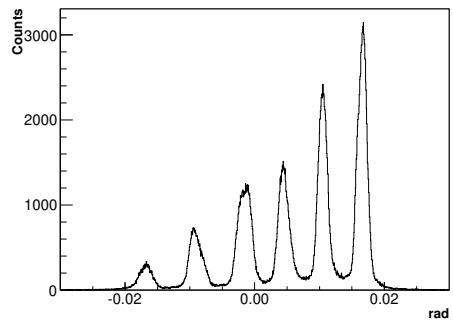

(b) Scattering variable ϕ histogram improved by the addition to ϕ of the polynomial $-0.042 \cdot \delta - 0.57 \cdot \delta^2 - 0.002 \cdot \theta + 0.8 \cdot \theta^2 + 0.18 \cdot y - 15.9 \cdot y^2 + 1.3 \cdot \theta \cdot \phi$.

Figure 3

HRS original database $T_{rightHRS_{4klmn}}$ that provide the value of the scattering variable ϕ are uncalibrated. To calibrate them we used eq. (31) and eq. (32), with $\phi' = \phi - P_\phi$. The database calibration was hence performed expressing $\phi - 0.042 \cdot \delta - 0.57 \cdot \delta^2 - 0.002 \cdot \theta + 0.8 \cdot \theta^2 + 0.18 \cdot y - 15.9 \cdot y^2 + 1.3 \cdot \theta \cdot \phi$ as a polynomial in the variables x_f, y_f, θ_f, and ϕ_f making use of the uncalibrated database $T_{rightHRS}$ by expressing the scattering variables δ, θ, and ϕ as: $\delta/\theta/\phi = \sum_{tuvz} T_{rightHRS_{1/2/4tuvz}} \cdot (x_f)^t \cdot (y_f)^u \cdot (\theta_f)^v \cdot (\phi_f)^z$, with t, u, v, and z integer numbers. After expanding the powers in the resulting polynomial, the terms $T'_{rightHRS_{4klmn}}$ of the calibrated database were obtained as the sums of all the coefficients of the terms proportional to $(x_f)^k \cdot (y_f)^l \cdot (\theta_f)^m \cdot (\phi_f)^n$ with k, l, m, and n integer numbers. Alternatively, one can just substitute the variable ϕ with the variable $\phi' = \phi - P_\phi$ in all the formulas of interest, like the one for the calculation of the binding energy. As quoted in section 4.2 this is equivalent to performing calculations using as a base the scattering coordinates instead of the focal plane coordinates.

Figure 4 shows the histograms of the variable $1+\delta-\frac{P_0}{P_c} \cdot \frac{1}{1+2 \cdot \frac{P_0}{M} \cdot \sin^2\left(\frac{\Theta}{2}\right)}$, with P_c the momentum of the central trajectory in the right HRS, P_0 the electron beam momentum, Θ the electron scattering angle, and M the mass of ^{12}C, obtained, during the elastic electron scattering calibration run, making use of the original right HRS database (Figure 4a) and of the database obtained after the calibration of the terms providing the scattering variable ϕ described above (Figure 4b). The plots in Figure 4 are disappointing, as one expects

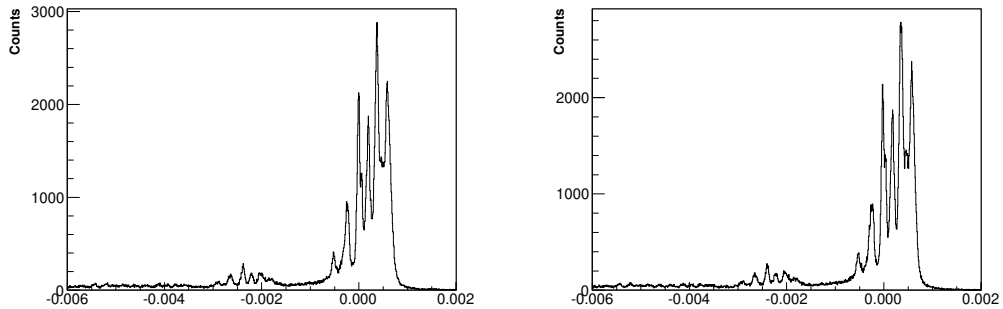

(a) Variable $1+\delta-\frac{P_0}{P_c}\cdot\frac{1}{1+2\cdot\frac{P_0}{M}\cdot\sin^2\left(\frac{\Theta}{2}\right)}$ histogram obtained with the right HRS original database.

(b) Variable $1+\delta-\frac{P_0}{P_c}\cdot\frac{1}{1+2\cdot\frac{P_0}{M}\cdot\sin^2\left(\frac{\Theta}{2}\right)}$ histogram obtained after calibrating, in the right HRS original database, the terms providing the scattering variable ϕ .

Figure 4

the elastic peak in these spectra to be centered around zero (see eq. (B.4)), with a very small FWHM due to the spectrometer's high resolution, and with possibly some smaller peaks present in these spectra at negative values corresponding to the energy levels of the first excited states of ^{12}C for which $1+\delta < \frac{P_0}{P_c}\cdot\frac{1}{1+2\cdot\frac{P_0}{M}\cdot\sin^2\left(\frac{\Theta}{2}\right)}$. As shown in Figure 4b the calibration of the scattering variable ϕ in equation (B.4) does not help much because the value $1+\delta$ is not very sensitive to the recoil factor $\frac{1}{1+2\cdot\frac{P_0}{M}\cdot\sin^2\left(\frac{\Theta}{2}\right)}$.

However, nearly miraculously, everything is settled by substituting the variable δ with the variable $\delta' = \delta - 0.031\cdot\phi$. Figure 5a shows the histogram of the variable $1+\delta'-\frac{P_0}{P_c}\cdot\frac{1}{1+2\cdot\frac{P_0}{M}\cdot\sin^2\left(\frac{\Theta}{2}\right)}-0.00027$, where the costant -0.00027 was added to position the elastic peak at zero in the spectrum. This mispositioning of the elastic peak is likely due to a percentage difference of the order of $2.7\cdot10^{-4}$ between the electron beam momentum and the right HRS central trajectory momentum, both nominally set at 1.85 GeV/c. Figure 5b is the histogram of fig 5a with the abscissa units multiplied by the factor 1850 (the value of the right HRS central trajectory momentum expressed in MeV/c), and with an ordinate logarithmic scale in order to show clearly the values of the energy levels of the ^{12}C excited states.

This example shows how powerful the method described in this paper to calibrate magnetic spectrometer databases is. Despite the dreadful starting point represented by the plots of Figure 4, the terms of the database that

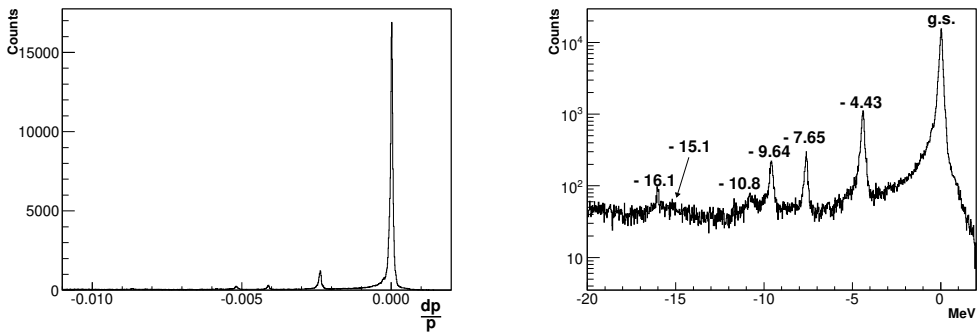

(a) (b)

Figure 5: (a): the histogram of Figure 4b after the substitution $\delta \rightarrow \delta' = \delta - 0.031 \cdot \phi$. (b): the same histogram as (a) but the abscissa units (MeV) and the ordinate scale (logarithmic).

provide the correct values of δ are simply obtained multiplying the terms of the right HRS original database that provide ϕ by the factor "- 0.031" and summing the new terms obtained this way to the terms of the right HRS original database that provide δ. A calculation that takes not more than 5-10 minutes even without the help of a computer. The false dependence on ϕ of the law $1 + \delta - \frac{P_0}{P_c} \cdot \frac{1}{1+2\cdot\frac{P_0}{M}\cdot\sin^2\left(\frac{\Theta}{2}\right)} = 0$ that signals the fact that the terms of the right HRS original database that provide δ are uncalibrated is evident from the plots of Figure 4 that show that the elastic peak is split into six peaks corresponding to the six values $\phi = constant_n$ of the spot centers of Figure 1. It has to be noted that the false dependence of the law $1+\delta-\frac{P_0}{P_c}\cdot\frac{1}{1+2\cdot\frac{P_0}{M}\cdot\sin^2\left(\frac{\Theta}{2}\right)} = 0$ is on ϕ despite the fact that the real uncalibrated scattering variable is δ. It has to be noted that, during experiment E94-107 analysis, the fact that the scattering variable δ, as provided by the right HRS original database, was uncalibrated was discovered through a dependence of the binding energies of the hypernuclei on ϕ in the form of the addition of the polynomial term $-4.72896\cdot\phi$ to the binding energy constant values. This polynomial term was eliminated with the substitution $\delta \rightarrow \delta' = \delta - 0.031 \cdot \phi$. See text from eq. (33) to eq. (41) for the method by which the coefficient "0.031" was determined from the acknowledgement of the dependence on the polynomial term $-4.72896 \cdot \phi$ of the binding energies as calculated through the right HRS original database.

6. Conclusions

A method to calibrate magnetic spectrometer databases based on the observation of false dependencies on scattering variables of physical laws has been shown. The physical laws involved are the independence on scattering variables of the energy levels of nuclei and/or hypernucei, the relationship between particle momentum and scattering angle in particle elastic scattering and so on. These false dependencies on scattering variables of physical laws appear if and only if the databases under study are uncalibrated. The quantitative study of these false dependencies allows us to calibrate databases very precisely. It can even allow us to perform measurements without explicitly calibrating the databases of the magnetic spectrometers involved although obviously a database calibration is always desirable. If physical law false dependencies on scattering variables do not appear, the databases under study are calibrated and no attempt to improve them should be pursued as it would generate physical law false dependencies on scattering variables making the dat bases concerned uncalibrated. Other methods to calibrate magnetic spectrometer databases exist (see for example [19]) and they can be used alternatively or complementarily to the method described in this paper. Whatever the method used, however, the result has to be the same: no false dependencies on scattering variables of physical laws should appear. The method described in this paper was used to calibrate the two High Resolution Spectrometers employed in experiment E94-107 allowing us to obtain sub-Mev resolutions. However, it can be generalized in order to calibrate any measurement instrument. This can be very useful if it is not possible to calibrate measurement instruments with samples of known values of the physical quantities concerned because of the intrinsic nature of the measurement involved.

Acknowledgments

This work was supported by U.S. Department Of Energy, Office of Science, Office of Nuclear Physics under contract DE-AC05-06OR23177, under which the Southeastern Universities Research Association (SURA) operates the Thomas Jefferson National Accelerator Facility, and by the Italian Istituto Nazionale di Fisica Nucleare.

Appendix A. Changes of numerical values of scattering variables and binding energies due to spectrometer database modifications

Let us suppose we have a spectrometer optical database $T^1_{e'}$ by which we determine the vector $\vec{Y}^1_{e'}$ whose components are the scattering variables of a particle e' ($\vec{Y}^1_{e'} \equiv \left(\delta^1_{e'}, y^1_{e'_0}, \theta^1_{e'_0}, \phi^1_{e'_0}\right)$) through the equation:

$$\vec{Y}^1_{e'} = T^1_{e'} \cdot \vec{X}_{e'} \tag{A.1}$$

where $\vec{X}_{e'}$ is the vector whose components are the particle e' coordinates and angles at the spectrometer focal plane ($\vec{X}_{e'} \equiv \left(x_{e'_f}, y_{e'_f}, \theta_{e'_f}, \phi_{e'_f}\right)$) and the superscript "1 " indicates that $Y^1_{e'}$ was derived through the tensor $T^1_{e'}$.

The explicit form of eq. (A.1) is:

$$Y^1_{e'_i} = \sum_{klmn} T^1_{e'_{iklmn}} \cdot (X_{e'_1})^k \cdot (X_{e'_2})^l \cdot (X_{e'_3})^m \cdot (X_{e'_4})^n \tag{A.2}$$

where $i = 1, 2, 3, 4$ and k, l, m, and n are integer numbers. Changing the spectrometer database means replacing the tensor $T^1_{e'}$ with a tensor $T^2_{e'}$. With this change, eq. (A.1) changes into:

$$\vec{Y}^2_{e'} = T^2_{e'} \cdot \vec{X}_{e'} = T^1_{e'} \cdot \vec{X}_{e'} + \Delta T^1_{e'} \cdot \vec{X}_{e'} = \vec{Y}^1_{e'} + \Delta \vec{Y}^1_{e'} \tag{A.3}$$

where we defined $\Delta T^1_{e'}$ as the tensor whose components are given by the expression:

$$\Delta T^1_{e'_{iklmn}} = T^2_{e'_{iklmn}} - T^1_{e'_{iklmn}} \tag{A.4}$$

and

$$\Delta \vec{Y}^1_{e'} = \Delta T^1_{e'} \cdot \vec{X}_{e'} \tag{A.5}$$

Defining I the unitary tensor and the tensor $S^1_{e'}$ as the inverse tensor of $T^1_{e'}$:

$$S^1_{e'} = (T^1_{e'})^{-1}; \quad S^1_{e'} \cdot T^1_{e'} = I \tag{A.6}$$

we have:

$$\vec{X}_{e'} = S^1_{e'} \cdot \vec{Y}^1_{e'} \tag{A.7}$$

and

$$\Delta\vec{Y}^1_{e'} = \Delta T^1_{e'} \cdot \vec{X}_{e'} = \Delta T^1_{e'} \cdot S^1_{e'} \cdot \vec{Y}^1_{e'} = U^1_{e'} \cdot \vec{Y}^1_{e'} \tag{A.8}$$

where we defined the tensor $U^1_{e'}$, that operates on the scattering coordinates $Y^1_{e'_i}$, as:

$$U^1_{e'} = \Delta T^1_{e'} \cdot S^1_{e'} \tag{A.9}$$

The explicit form of eq. (A.8) is:

$$\begin{aligned}\Delta Y^1_{e'_i} = \sum_{pqrs} \Delta T^1_{e'_{ipqrs}} \cdot & \left(\sum_{t,u,v,z} S^1_{e'_{1tuvz}} \cdot \left(Y^1_{e'_1}\right)^t \cdot \left(Y^1_{e'_2}\right)^u \cdot \left(Y^1_{e'_3}\right)^v \cdot \left(Y^1_{e'_4}\right)^z \right)^p \cdot \\ & \left(\sum_{t,u,v,z} S^1_{e'_{2tuvz}} \cdot \left(Y^1_{e'_1}\right)^t \cdot \left(Y^1_{e'_2}\right)^u \cdot \left(Y^1_{e'_3}\right)^v \cdot \left(Y^1_{e'_4}\right)^z \right)^q \cdot \\ & \left(\sum_{t,u,v,z} S^1_{e'_{3tuvz}} \cdot \left(Y^1_{e'_1}\right)^t \cdot \left(Y^1_{e'_2}\right)^u \cdot \left(Y^1_{e'_3}\right)^v \cdot \left(Y^1_{e'_4}\right)^z \right)^r \cdot \\ & \left(\sum_{t,u,v,z} S^1_{e'_{4tuvz}} \cdot \left(Y^1_{e'_1}\right)^t \cdot \left(Y^1_{e'_2}\right)^u \cdot \left(Y^1_{e'_3}\right)^v \cdot \left(Y^1_{e'_4}\right)^z \right)^s = \\ & \sum_{k,l,m,n} U^1_{e'_{iklmn}} \cdot \left(Y^1_{e'_1}\right)^k \cdot \left(Y^1_{e'_2}\right)^l \cdot \left(Y^1_{e'_3}\right)^m \cdot \left(Y^1_{e'_4}\right)^n \end{aligned} \tag{A.10}$$

where, similarly to eq. (A.2), $i = 1, 2, 3, 4$; k, l, m, and n are integer numbers as well as p, q, r, s , t, u, v, and z, and $U^1_{e'_{iklmn}}$ are the elements of the tensor $U^1_{e'}$ equal to the sum of the coefficients of the terms proportional to $\left(Y^1_{e'_1}\right)^k \cdot \left(Y^1_{e'_2}\right)^l \cdot \left(Y^1_{e'_3}\right)^m \cdot \left(Y^1_{e'_4}\right)^n$ in the first four rows of eq. (A.10).

In the first order approximation eq. (A.10) reduces to:

$$\Delta Y^1_{e'_i} = \sum_{k=1,4} \Delta T^1_{e'_{ik}} \cdot \left(\sum_{j=1,4} S^1_{e'_{kj}} \cdot Y^1_{e'_j} \right) = \sum_{j=1,4} U^1_{e'_{ij}} Y^i_{e'_j} \tag{A.11}$$

with $U^1_{e'_{ij}} = \sum_{k=1,4} \Delta T^1_{e'_{ik}} \cdot S^1_{e'_{kj}}$.

In eq. (A.10) we were hence able to express the numerical change $\Delta Y^1_{e'_i}$, which the ith scattering coordinate $Y^1_{e'_i}$ of the particle e' is subjected due

to the change of the spectrometer optical database from $T^1_{e'}$ to $T^2_{e'}$, as a polynomial in the scattering coordinates $Y^1_{e'_i}$ themselves.

Combining eq. (A.3) with eq. (A.10) we have:

$$Y^2_{e'_i} = Y^1_{e'_i} + P(\delta^1_{e'}, y^1_{e'_0}, \theta^1_{e'_0}, \phi^1_{e'_0}) \tag{A.12}$$

with $P(\delta^1_{e'}, y^1_{e'_0}, \theta^1_{e'_0}, \phi^1_{e'_0})$ a polynomial in the scattering coordinates $\delta^1_{e'} \equiv Y^1_{e'_1}$, $y^1_{e'_0} \equiv Y^1_{e'_2}$, $\theta^1_{e'_0} \equiv Y^1_{e'_3}$, and $\phi^1_{e'_0} \equiv Y^1_{e'_4}$.

Binding energies of nucleus/hypernucleus energy levels are experimentally determined by measuring scattering coordinates of particles detected in coincidence. The way they were determined in the case of the coordinate system used in the experiment E94-107 where scattered electrons, e', and produced kaons, k, were detected in coincidence is shown in Appendix Appendix C. Here it suffices to say that the most generic form of eq. (27) is:

$$E_{bind_n}\left(\vec{Y}_{e'}, \vec{Y}_k\right) = constant_n$$

with $\vec{Y}_k$ the vector whose components are the scattering variables of the particle k. It is straightforward to understand the effect, on the numerical calculation of the binding energies, of a change in a spectrometer optical database. Just limiting, for the sake of simplicity but without loss of generality, Taylor series to zero and first order terms, we have, in fact, that when switching from a database $T^1_{e'}$ to a database $T^2_{e'}$ and, as a consequence, switching from the scattering coordinates $Y^1_{e'_i}$ to the coordinates $Y^2_{e'_i} = Y^1_{e'_i} + \Delta Y^1_{e'_i}$ of the particle e', while keeping unchanged the database T^1_k of the spectrometer that detects the particle k and hence keeping unchanged the scattering coordinates $Y^1_{k_i}$, the numerical expression for the binding energy $E_{bind_n}\left(\vec{Y}^1_{e'}, \vec{Y}^1_k\right)$ for the generic energy level n changes into $E_{bind_n}\left(\vec{Y}^2_{e'}, \vec{Y}^1_k\right)$ equal to:

$$E_{bind_n}\left(\vec{Y}^2_{e'},\vec{Y}^1_k\right) = E_{bind_n}\left(\vec{Y}^1_{e'} + \Delta\vec{Y}^1_{e'},\vec{Y}^1_k\right) =$$

$$E_{bind_n}\left(\vec{Y}^1_{e'},\vec{Y}^1_k\right) + \sum_{i=1,4} \Delta Y^1_{e'_i} \cdot \left.\frac{\partial E_{bind_n}\left(\vec{Y}_{e'},\vec{Y}_k\right)}{\partial Y_{e'_i}}\right|_{\vec{Y}_{e'}=\vec{Y}^1_{e'}} =$$

$$E_{bind_n}\left(\vec{Y}^1_{e'},\vec{Y}^1_k\right) +$$

$$\sum_{iklmn} U^1_{e'_{iklmn}} \cdot \left(Y^1_{e'_1}\right)^k \cdot \left(Y^1_{e'_2}\right)^l \cdot \left(Y^1_{e'_3}\right)^m \cdot \left(Y_{e'_4}\right)^n \cdot \left.\frac{\partial E_{bind_n}\left(\vec{Y}_{e'},\vec{Y}_k\right)}{\partial Y_{e'_i}}\right|_{\vec{Y}_{e'}=\vec{Y}^1_{e'}} \tag{A.13}$$

where $\left.\frac{\partial E_{bind_n}}{\partial Y_{e'_i}}\right|_{\vec{Y}_{e'}=\vec{Y}^1_{e'}}$ are the values of the derivative of $E_{bind_n}\left(\vec{Y}_{e'},\vec{Y}_k\right)$ with respect to $Y_{e'_i}$ at $\vec{Y}_{e'} = \vec{Y}^1_{e'}$ ($i = 1, 2, 3, 4$), and where we used eq. (A.10) for $\Delta Y^1_{e'_i}$.

The derivatives $\left.\frac{\partial E_{bind_n}}{\partial Y_{e'_i}}\right|_{\vec{Y}_{e'}=\vec{Y}^1_{e'}}$ are in principle functions of $\delta^1_{e'} \equiv Y^1_{e'_1}$, $y^1_{e'_0} \equiv Y^1_{e'_2}$, $\theta^1_{e'_0} \equiv Y^1_{e'_3}$, and $\phi^1_{e'_0} \equiv Y^1_{e'_4}$:

$$\left.\frac{\partial E_{bind_n}}{\partial Y_{e'_i}}\right|_{\vec{Y}_{e'}=\vec{Y}^1_{e'}} = f_{e'_i}(\vec{Y}^1_{e'}) \equiv f_{e'_i}(\delta^1_{e'}, y^1_{e'_0}, \theta^1_{e'_0}, \phi^1_{e'_0}) \tag{A.14}$$

However, they are nearly constant as deduced developing them in a MacLaurin series. For example, for $f_{e'_1} \equiv f_{e'_\delta}$ we have:

$$\begin{aligned}\left.\frac{\partial E_{bind_n}}{\partial \delta_{e'}}\right|_{\vec{Y}_{e'}=\vec{Y}^1_{e'}} &= f_{e'_\delta}(\delta^1_{e'}, y^1_{e'_0}, \theta^1_{e'_0}, \phi^1_{e'_0}) = f_{e'_\delta}(0,0,0,0) + \\ &\Delta\delta^1_{e'} \cdot \left.\frac{\partial f_{e'_\delta}(\delta^1_{e'}, y^1_{e'_0}, \theta^1_{e'_0}, \phi^1_{e'_0})}{\partial \delta^1_{e'}}\right|_{\vec{Y}^1_{e'}=\vec{0}} + \\ &\Delta y^1_{e'_0} \cdot \left.\frac{\partial f_{e'_\delta}(\delta^1_{e'}, y^1_{e'_0}, \theta^1_{e'_0}, \phi^1_{e'_0})}{\partial y^1_{e'_0}}\right|_{\vec{Y}^1_{e'}=\vec{0}} + \\ &\Delta\theta^1_{e'_0} \cdot \left.\frac{\partial f_{e'_\delta}(\delta^1_{e'}, y^1_{e'_0}, \theta^1_{e'_0}, \phi^1_{e'_0})}{\partial \theta^1_{e'_0}}\right|_{\vec{Y}^1_{e'}=\vec{0}} + \\ &\Delta\phi^1_{e'_0} \cdot \left.\frac{\partial f_{e'_\delta}(\delta^1_{e'}, y^1_{e'_0}, \theta^1_{e'_0}, \phi^1_{e'_0})}{\partial \phi^1_{e'_0}}\right|_{\vec{Y}^1_{e'}=\vec{0}} + \ldots\end{aligned} \tag{A.15}$$

where $\vec{0}$ is the vector with all its components equal to zero. From eq. (C.2-C.5) we can deduce that, in the kinematics adopted by the experiment E94-107, defining $P_{e'_c}$, M_{hyp}, and M_{tar} the central trajectory momentum of the spectrometer that detected the particles e', the mass of the hypernucleus produced, and the mass of the target respectively, considering that the momentum acceptance of the High Resolution Spectrometers employed was 8%, the ratio between $\Delta\delta^1_{e'} \cdot \frac{\partial f_{e'_\delta}(\delta^1_{e'}, y^1_{e'_0}, \theta^1_{e'_0}, \phi^1_{e'_0})}{\partial \delta^1_{e'}}\Big|_{\vec{Y}^1_{e'}=\vec{0}}$ and $f_{e'_\delta}(0,0,0,0)$ was not bigger than $0.04 \cdot \frac{P_{e'_c} \cdot M_{tar}}{M^2_{hyp}} \approx 5 \cdot 10^{-3}$ while the other terms in the Maclaurin series of eq. (A.15) were completely negligible.

Defining the (nearly constant) coefficients $C^1_{e'_{iklmn}}$ as:

$$C^1_{e'_{iklmn}} = U^1_{e'_{iklmn}} \cdot \frac{\partial E_{bind_n}\left(\vec{Y}_{e'}, \vec{Y}_k\right)}{\partial Y_{e'_i}}\Bigg|_{\vec{Y}_{e'}=\vec{Y}^1_{e'}}$$

eq. (A.13) can be written as:

$$\begin{aligned} E_{bind_n}\left(\vec{Y}^2_{e'}, \vec{Y}^1_k\right) &= E_{bind_n}\left(\vec{Y}^1_{e'}, \vec{Y}^1_k\right) + \\ \sum_{iklmn} C^1_{e'_{iklmn}} \cdot \left(Y^1_{e'_1}\right)^k \cdot \left(Y^1_{e'_2}\right)^l \cdot \left(Y^1_{e'_3}\right)^m \cdot \left(Y_{e'_4}\right)^n &= \\ E_{bind_n}\left(\vec{Y}^1_{e'}, \vec{Y}^1_k\right) + P^1_{E_{bind_n}}(\delta^1_{e'}, y^1_{e'_0}, \theta^1_{e'_0}, \phi^1_{e'_0}) & \end{aligned} \tag{A.16}$$

with $P^1_{E_{bind_n}}(\delta^1_{e'}, y^1_{e'_0}, \theta^1_{e'_0}, \phi^1_{e'_0})$ a polynomial in scattering coordinates.

If in eq. (A.15) $\Delta\delta^1_{e'} \cdot \frac{\partial f_{e'_\delta}(\delta^1_{e'}, y^1_{e'_0}, \theta^1_{e'_0}, \phi^1_{e'_0})}{\partial \delta^1_{e'}}\Big|_{\vec{Y}^1_{e'}=\vec{0}}$ cannot be considered negligible, the coefficients $C^1_{e'_{1klmn}}$ in eq. (A.16) have to be changed into:

$$C^1_{e'_{1iklmn}} = U^1_{e'_{1klmn}} \cdot \left(f_{e'_\delta}(0,0,0,0) + \Delta\delta^1_{e'} \cdot \frac{\partial f_{e'_\delta}(\delta^1_{e'}, y^1_{e'_0}, \theta^1_{e'_0}, \phi^1_{e'_0})}{\partial \delta^1_{e'}}\Bigg|_{\vec{Y}^1_{e'}=\vec{0}} \right) \tag{A.17}$$

Appendix B. Analytical expression of the particle elastic scattering variables in the coordinate system of the Hall A High Resolution Spectrometers

In the experiment E94-107 two High Resolution Spectrometers (HRS) were used. In the coordinate system conventionally used by the software

analyzing each single HRS data point, the coordinate x represents the displacement, in the dispersive plane, of the particle trajectory with respect to the reference (central) trajectory, the angle θ is the tangent of the angle the particle trajectory makes in the dispersive plane with respect to the central trajectory, and y and ϕ are equivalent to x and θ in the transverse plane. δ is the percentage difference between the particle momentum and the spectrometer central trajectory momentum. For the HRS's x is in the vertical direction and y is in the horizontal direction. The orientation of the x; y; and z-axes are such that $\hat{z} = \hat{x} \times \hat{y}$. As in a spectrometer the deviations of particle parameters with respect to the corresponding central trajectory are usually small, the angles that define particle trajectories with respect to the spectrometer central trajectory are very small and nearly numerically equal to their tangents. For this reason, for the sake of simplicity, we refer to θ and ϕ as angles, although they are actually the tangents of the angles with which they are identified. Inside each HRS, the particle momentum coordinates P_x, P_y, and P_z with respect to the HRS central trajectory are provided by the equations:

$$\begin{aligned} P_x &= P_c \cdot (1+\delta) \cdot sin(\theta) \\ P_y &= P_c \cdot (1+\delta) \cdot cos(\theta) \cdot \sin(\phi) \\ P_z &= P_c \cdot (1+\delta) \cdot cos(\theta) \cdot \cos(\phi) \end{aligned} \tag{B.1}$$

At the scattering point ($\theta = \theta_0; \phi = \phi_0$) the particle momentum components in the laboratory frame are:

$$\begin{aligned} P_x &= P_c \cdot (1+\delta) \cdot sin(\theta_0) \\ P_y &= P_c \cdot (1+\delta) \cdot cos(\theta_0) \cdot \sin(\phi_0 + \phi_c) \\ P_z &= P_c \cdot (1+\delta) \cdot cos(\theta_0) \cdot \cos(\phi_0 + \phi_c) \end{aligned} \tag{B.2}$$

where ϕ_c is the angle between the HRS axis and the beam line (for each HRS θ_c , i.e. the angle between its axis and the horizontal plane, can be assumed equal to zero).

In elastic scattering, the relationship between primary (E_0) and scattered (E') particle energies is expressed by the equation:

$$E' = \frac{E_0}{1 + 2 \cdot \frac{E_0}{M} \cdot \sin^2\left(\frac{\Theta}{2}\right)} \tag{B.3}$$

where M is the mass of the nucleus off which the particles scatter. In experiment E94-107, the primary beam consisted in relativistic electrons, for which (in units where c = 1) $E' \approx P_c \cdot (1+\delta)$ and $E_0 \approx P_0$, with P_0 the primary electron momentum and hence eq. (B.3) transforms into:

$$P_c \cdot (1+\delta) = \frac{P_0}{1 + 2 \cdot \frac{P_0}{M} \cdot \sin^2\left(\frac{\Theta}{2}\right)} \tag{B.4}$$

with

$$\Theta = arccos\left(\frac{P_x \cdot P_{0_x} + P_y \cdot P_{0_y} + P_z \cdot P_{0_z}}{P_c \cdot (1+\delta) \cdot P_0}\right) \tag{B.5}$$

Appendix C. Analytical expression of the binding energies of the hypernuclei produced in experiment E94-107 in the coordinate system of the Hall A High Resolution Spectrometers

The binding energies of the ground and excited states of the hypernuclei produced by an electron scattering off nuclei of atomic number Z and mass number A

$$^{A}(Z)\left(e, e'k^+\right)^{A}_{\Lambda}(Z-1) \tag{C.1}$$

are calculated as:

$$E_{bind} = -\sqrt{(E_m)^2 - \left(\vec{P}_m\right)^2} + M_{residue} + M_\Lambda \tag{C.2}$$

where $M_{residue}$ is the mass of the residual nucleus, that is of the nucleus with $A-1$ nucleons and $Z-1$ protons, M_Λ is the Λ mass, and E_m and $\vec{P}_m$ respectively are the missing energy and the missing momentum, equal to:

$$\begin{aligned} E_m &= E_0 + M_{target} - E_{e'} - E_k \\ \vec{P}_m &= \vec{P}_0 - \vec{P}_{e'} - \vec{P}_k \end{aligned} \tag{C.3}$$

with M_{target} the target mass, E_0, $E_{e'}$, and E_k the energies of the incident electron, of the scattered electron, and of the produced kaon respectively, and $\vec{P}_0$, $\vec{P}_{e'}$, and $\vec{P}_k$ the momenta of the incident electron, of the scattered electron, and of the produced kaon respectively.

Experiment E94-107 employed two High Resolution Spectrometers, one for the detection of the scattered electrons, the other for the detection of the kaons (see section 2). Identifying with the subscripts e' the coordinates and parameters relative to the spectrometer detecting scattered electrons and with the subscripts k the corresponding values of the spectrometer detecting produced kaons, we have (see eq. (B.2) for the meaning of the variables):

$$\begin{aligned} P_{e'_x} &= P_{e'_c} \cdot (1+\delta_{e'}) \cdot \sin(\theta_{e'_0}) \\ P_{e'_y} &= P_{e'_c} \cdot (1+\delta_{e'}) \cdot \cos(\theta_{e'_0}) \cdot \sin(\phi_{e'_0} + \phi_{e'_c}) \\ P_{e'_z} &= P_{e'_c} \cdot (1+\delta_{e'}) \cdot \cos(\theta_{e'_0}) \cdot \cos(\phi_{e'_0} + \phi_{e'_c}) \end{aligned} \tag{C.4}$$

$$\begin{aligned} P_{k_x} &= P_{k_c} \cdot (1+\delta_k) \cdot \sin(\theta_{k_0}) \\ P_{k_y} &= P_{k_c} \cdot (1+\delta_k) \cdot \cos(\theta_{k_0}) \cdot \sin(\phi_{k_0} + \phi_{k_c}) \\ P_{k_z} &= P_{k_c} \cdot (1+\delta_k) \cdot \cos(\theta_{k_0}) \cdot \cos(\phi_{k_0} + \phi_{k_c}) \end{aligned} \tag{C.5}$$

References

[1] F. Garibaldi, S. Frullani, P. Markowitz, and J. LeRose (spokespersons), JLab Experiment E94-107 high-resolution 1p shell hypernuclear spectroscopy (1994).

[2] M. Iodice et al., Phys Rev. Lett 99 (2007), 052501.

[3] F. Cusanno et al., Phys. Rev. Lett. 103 (2009), 202501.

[4] G.M. Urciuoli et al., Phys. Rev. C 91 (2015), 034308.

[5] Y.-C. Chao, P. Chevtsov, A. Day, A. P. Freyberger, R. Hicks, M. Joyce, and J.-C. Denard, "Energy spread monitoring for the JLAB experimental program: synchrotron light interferometers, optical transition radiation monitors and wire scanners." in Beam instrumentation workshop 2004, edited by T. Shea and R. Coles Sibley III (AIP Conference Proceedings No. 732, 2004) p. 120.

[6] G. A. Krafft, J.-C. Denard, R. W. Dickson, R. Kazimi, V. A. Lebedev, and M. G. Tiefenback, "Measuring and controlling the energy spread

in CEBAF," in Proceedings of the XX International Linac Conference, Monterey, California, USA, edited by A. W. Chao (SLAC-R-561, eConf:C000821, 2000) p. 721, arXiv:physics/0009087.

[7] M. Iodice et al. Nucl. Intrum. Methods Phys. Res. A 411, 223 (1998).

[8] E. Cisbani et al., Nucl. Intrum. Methods Phys. Res. A 496, 305 (2003).

[9] L. Lagamba et al., Nucl. Intrum. Methods Phys. Res. A 471, 325 (2001).

[10] M. Iodice et al., Nucl. Intrum. Methods Phys. Res. A 553, 231 (2005).

[11] F. Garibaldi et al., Nucl. Intrum. Methods Phys. Res. A 502, 117 (2003).

[12] F. Cusanno et al., Nucl. Intrum. Methods Phys. Res. A 502, 251 (2003).

[13] G. M. Urciuoli et al., Nucl. Intrum. Methods Phys. Res. A 612, 56 (2009).

[14] J. Alcorn et al., Nucl. Intrum. Methods Phys. Res. A 522, 294 (2004).

[15] P. Brindza et al., IEEE TRANSACTION ON APPLIED SUPERCONDUCTIVITY 11(1): 1594-1596 (2001).

[16] G. M. Urciuoli et al., Nucl. Phys. A 691, 43c (2001).

[17] "A Proposal for TWO SEPTUM MAGNETS FOR FORWARD ANGLE PHYSICS IN HALL A AT TJNAF"', https://www.ge.infn.it/jlab12/files/Two-Sptum-magnets-for-forward-angle-physics-in-Hall-A-at-TJNAF.pdf, last accessed on October 28 2018.

[18] K.L. Brown, SLAC Report 75 (1970), revised edition, 1982, unpublished.

[19] "Optics Calibration of the Hall A High Resolution Spectrometers using the new optimizer" https://hallaweb.jlab.org/publications/Technotes/files/2002/02-012.pdf (2002), last accessed on October 28 2018.